Relationship between optical wiring conditions and MPI degradation

Chisato Fukai, Kazuhide Nakajima, Tomoya Shimizu, Takashi Matsui, Yukihiro Goto, and Toshio Kurashima
NTT Access Network Service Systems Laboratories, NTT Corporation.
1-7-1 Hanabatake, Tsukuba, Ibaraki 305-0805, Japan
Tel: +81-29-868-6410, Fax: +81-29-868-6142, E-mail: chisato@ansl.ntt.co.jp

Abstract: Optical wiring conditions are investigated numerically and experimentally with a viewpoint of MPI induced transmission performance degradation. We reveal the impact of the interval of the bending portion on MPI degradation for the first time.

OCIS codes: (060.2430) Fibers, single-mode; (060.2400) Fiber properties

1. Introduction

Bending-loss insensitive fibers (BIFs) have been developed for constructing future optical access networks effectively and economically [1]. It is very important that the optical fiber used in the fiber-to-the-home (FTTH) network has good transmission performance under bending conditions such as tight 90-degree corners, corners under load, and excess cable storage in small spaces [2, 3]. Recently, multipath interference (MPI), which is a transmission performance parameter, has been reported in BIFs [4, 5]. MPI, which is caused by a beat between a signal and a weak replica, can severely degrade system performance. In access networks that employ BIFs, there is concern that reflection at a fiber connection and a higher order mode at a signal wavelength shorter than the cable cutoff wavelength could induce a weak replica, and thus worsen the MPI. MPI has been studied in fibers bent with tight 90-degree corners and with multiple staples [4]. However, the relationship between MPI degradation and macrobending loss remains unclear.

In this paper, we discuss the relationship between MPI degradation and macrobending losses in BIFs and a single-mode fiber (SMF) both numerically and experimentally. We also examine the effect of the longitudinal distribution of the bending point on the MPI characteristics. Finally, we discuss the applicability of BIF for FTTH /indoor wiring application with respect to the MPI characteristics.

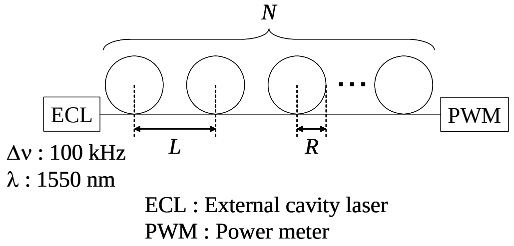

Fig. 1. Experimental setup.

2. Results and discussion

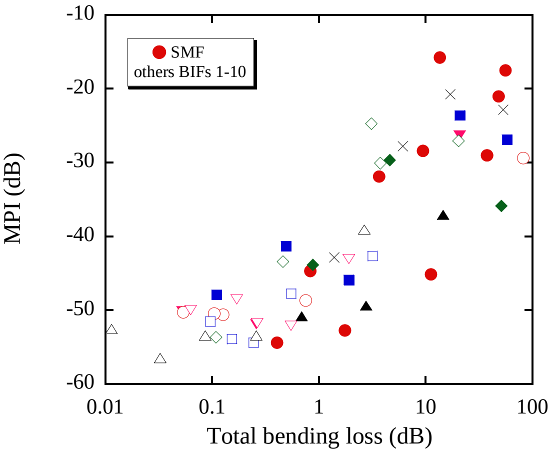

Fig. 2. Relationship between total bending loss and MPI.

We measured the MPI and macrobending losses of ten BIFs and an SMF. Figure 1 shows our experimental setup. We used an external cavity laser (ECL) with a linewidth Δν of 100 kHz and a power meter (PWM). The measurement wavelength λ was 1550 nm. The test fibers were fixed with a bend of radius *R*, number of turns *N*, and interval *L*. We evaluated the MPI using the peak-to-peak value of the power received by the PWM [4]. Figure 2 shows the relationship between the total bending losses and the MPI when *N* and *L* were 10 turns and 0 cm, respectively. This means that 10 turns of the test fiber were continuously wound with a radius of *R* in one bending part. The closed circles show results for the SMF, and the other symbols show the results for ten BIFs. For this measurement, we used high delta, trench, and hole assisted BIFs [1, 6]. Figure 2 reveals that abrupt MPI degradation is observed as the total bending loss increases above 1 dB. We also found that this trend was independent of the fiber type. We considered this to be because the leaked signal caused by bending is reflected from the boundary between the cladding and the fiber coating, and interferes with the signal into the core. The whispering gallery mode [7] might cause the fluctuation in the MPI values particularly when the bending loss becomes 1 dB or more. Figure 2 also reveals that the MPI was about -50 dB regardless of the bending losses when the total bending losses were less than 1 dB. In our measurement system, the MPI measurement limit was about -50 dB. Therefore, we thought that the MPI for the slight macrobending losses was fixed at that value.

The MPI induced analog transmission degradation can be evaluated by taking account of the relationship with relative intensity noise (RIN) [8] in terms of carrier to noise ratio (CNR) degradation [9]. As regards digital transmission, the MPI induced degradation can be considered as a power penalty [10]. These relationships can be expressed as follows.

$$CNR(linear) = \frac{m^2(\rho P_0)^2}{\left[2q\rho P_0 + i_n{}^2 + RIN(\rho P_0)^2\right]2B} \tag{1}$$

$$Power\quad penalty\quad (dB) = -10\log\left[1-(MPI/2)Q^2\right] \tag{2}$$

Here, *m* is the optical modulation index, ρ is the photodetector responsitivity, P_0 is the received optical power, *q* is the electron charge, i_n is the receiver thermal current, and *B* is the channel bandwidth.

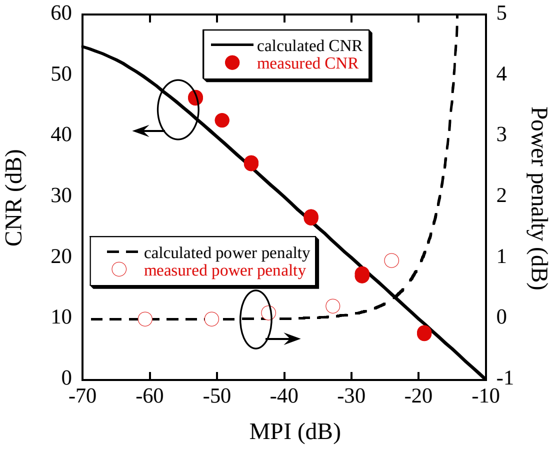

Fig. 3. CNR and power penalty at each MPI.

Figure 3 shows our experimental results for the MPI induced CNR degradation and power penalty. The closed and open circles show the measured CNR and power penalty, respectively. The solid and dashed lines show the respective calculated results. We set *m*, ρ, P_0, *q*, i_n, and *B* at 0.035, 0.95 A/W, 0 dBm, 1.6 × 10^{-19} C, 5 pA/$\sqrt{\ }$Hz, 4 MHz, respectively. We also adapted a Q value of 6 for a BER of 10^{-9}. We assumed a laser linewidth of 10 MHz and an electrical frequency of 91.25 MHz. For the measurement, we used an MPI source that consisted of two isolators and one optical attenuator between two power couplers [8]. Figure 3 shows that the measured and calculated results are in good agreement. As an MPI of -50 dB resulted in a bending loss of less than 1 dB as shown in Fig. 2, we can expect to obtain a CNR of about 40 dB and a power penalty of around 0 dB. In the digital transmission, although the power penalty increases rapidly when the MPI exceeds -20 dB, the power penalty for an MPI of less than about -30 dB is around 0 dB. By contrast, we found that the CNR in the analog transmission decreases linearly as the MPI degrades. Therefore, we can assume that the bending loss of 1 dB is the threshold for preventing MPI degradation and for maintaining the good transmission performance in a transmission network installed under tight bending conditions.

We then investigated the impact of the *L* value on the MPI characteristics. We used a high delta type fiber as the test sample and adopted a bending radius *R* so that the bending loss became 1 dB/turn. *N* was maintained at 10 turns.

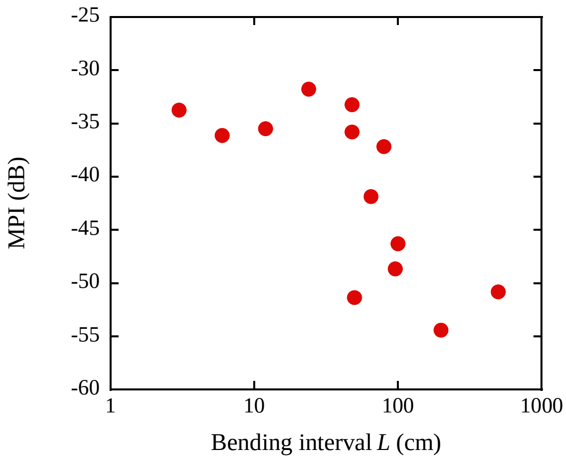

Fig. 4. Measured MPI at each bending interval.

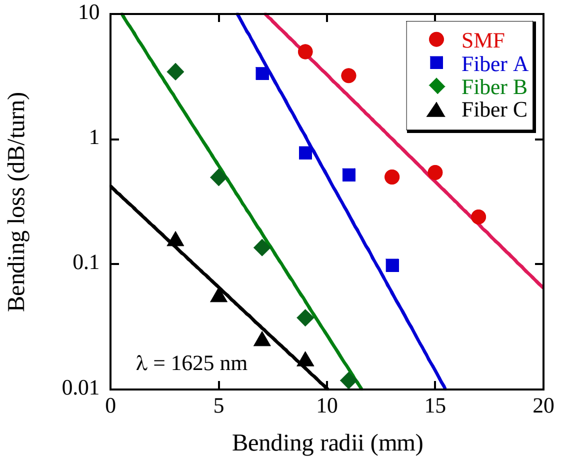

Fig. 5. Bending loss characteristics in some optical fibers.

Therefore, the total bending loss in this experimental setup was constant at 10 dB. Figure 4 shows the measured MPI at each *L*. We found that the MPI degrades to -35 dB when *L* is less than 100 cm. However, Fig. 4 also reveals that we can disregard the MPI degradation caused by tight bending when *L* is more than 100 cm. This means that even if the total bending loss in 1 route is 10 dB, the MPI degradation can be controlled by maintaining the bending loss at less than 1 dB and the interval at more than 100 cm.

Finally, we investigate the applicability of the BIFs from the standpoint of bending induced MPI degradation. Figure 5 shows example bending loss characteristics in some optical fibers. The symbols and solid lines show the measured and best-fitted results, respectively. Here, Fibers A, B, and C were high delta, trench, and hole assisted type fibers, respectively. We assumed two considerations. The first consideration corresponds to storage in an FTTH plant, and we assumed an allowable bending radius of 15 mm. The second consideration relates to indoor wiring, and we assumed a required bending radius of 5 mm with a view to realizing ease of handling [2]. Table 1 summarizes the applicability of the BIFs to optical storage and 90-degree corners shown in Fig. 5. Here, we assumed the maximum bending loss at 1 bend to be 1 dB taking account of the influence on the MPI. As regards storage, Table 1 confirms that the allowable number of turns is restricted to 1 for SMF. But, it can be relaxed to more than 100 turns when utilizing Fibers B and C. With respect to the allowable number of 90-degree corners, Table 1 confirms that Fiber B can be used for indoor wiring with 5 mm radius bend though the SMF and Fiber A are unusable. Moreover, Fiber C is more suitable for indoor wiring application because it allows the 50 or more tight bended corners. These results show BIFs can provide flexible indoor wiring by increasing the number of allowable corners.

Table 1. Applicability of BIFs to optical storage and 90-degree corners.

	SMF	Fiber A	Fiber B	Fiber C
Allowable number of turns for storage with 15 mm radius	1	70	>100	>100
Allowable number of 90-degree corners for indoor wiring with 5 mm radius	0	0	6	>50

3. Conclusion

We confirmed the relationship between bending loss and MPI characteristics both numerically and experimentally. We also revealed the impact of the interval of the bending portion on MPI degradation for the first time. We showed that bending induced MPI degradation can be ignored when the total bending loss in one bending part, which has an interval of more than 100 cm, is less than 1 dB. Our results can be used to consider the applicability of various BIFs for FTTH and/or indoor wiring use.

4. References

[1] K. Himeno, S. Matsuo, N. Guan, and A. Wada, “Low-bending–loss single-mode fibers for fiber-to-the-home,” J. Lightwave Technol., vol. 23, no. 11, pp. 3494-3499, 2005.

[2] J. Zhou, K. Nakajima, K. Tajima, K. Hogari, and K. Sato, “Application of hole-assisted type PCF with good bending loss performance,” 52nd IWCS, Philadelphia, PA, pp. 48-52, 2003.

[3] D. Z. Chen, W. R. Belben, J. B. Gallup, C. Mazzali, P. Dainese, and T. Rhyne, “Requirements for bend insensitive fibers for Verizon’s FiOS and FTTH applications,” OFC/NFOEC 2009, San Diego, CA, paper NTuC2, Feb., 2008.

[4] D. Z. Chen, V. X. Jain, R. C. Ditmore, G. N. Bell, D. Boivin, L. A. Montmorillon, L. Provost, and P. Sillard, “Testing MPI threshold in bend insensitive fiber using coherent peak-to-peak power method,” OFC/NFOEC 2009, San Diego, CA, paper NTuC5, March, 2009.

[5] M. J. Li, X. Chen, P. Dainese, J. J. Englebert, C. Saravanos, D. Z. Chen, V. X. Jain, R. C. Ditmore, and G. N. Bell, “Statistical analysis of MPI in bend-insensitive fibers,” OFC/NFOEC 2009, San Diego, CA, paper OTuL1, March, 2009.

[6] K. Nakajima, T. Shimizu, C. Fukai, T. Kurashima, and M. Shimizu, “Single-mode hole-assisted fiber with low bending loss characteristics,” to be published in IWCS 2009.

[7] A. J. Harris and P. F. Castle, “Bend loss measurements on high numerical aperture single-mode fibers as a function of wavelength and bend radius,” J. Lightwave Technol., vol. LT-4, no. 1, pp. 34-40, 1986.

[8] C. R. S. Fludger and R. J. Mears, “Electrical measurements of multipath interference in distributed Raman amplifiers,” J. Lightwave Technol., vol. 19, no. 4, pp. 536-545, 2001.

[9] Q. Shi, R. S. Burroughs, and D. Lewis, “An alternative model for laser clipping-induced nonlinear distortion for analog Lightwave CATV systems,” IEEE Photon. Technol. Lett., vol. 4, no. 7, pp. 784-787, 1992.

[10] H. Takahashi, K. Oda, and H. Toba, “Impact of crosstalk in an arrayed-waveguide multiplexer on *N* x *N* optical interconnection,” J. Lightwave Technol., vol. 14, no. 6, pp. 1097-1105, 1996.